Guarding a Territory Against an Intelligent Intruder: Strategy Design and Experimental Verification

Han Fu and Hugh H.-T. Liu, *Member, IEEE*

***Abstract*—This article designs and tests a dominant region based strategy for a group of defenders to intercept an intruder before it enters a target area. The intruder is intelligent in the sense that it makes decisions based on the defenders' strategies instead of following a predefined path, making the problem a differential game. When the intruder moves slower than the defenders, the optimal strategies are solved from a geometric concept called the dominant region. These strategies are then extended into the case where the intruder travels faster. Crazyflie 2.1 is used as an experimental platform to test the proposed strategy. For fixed defender locations, a barrier line can be found such that the intruder is guaranteed to be captured outside the target area if it starts beyond.**

***Index Terms*—Counter unmanned aerial vehicle (UAV), Crazyflie, differential game, dominant region (DR).**

I. Introduction

As RESEARCH efforts and developments in unmanned aerial vehicles (UAVs) increase, concerns about the potential security threats also grow. Drones have been reported shown up in prohibited or sensitive areas, such as government buildings, military bases, and airports. For example, in 2015, a drone crashed near the White House. In 2018, the U.K. Airprox Board reported that a drone intentionally crashed into an aircraft. The number of near misses between drones and aircraft has risen from 6 events to 93 during 2014 to 2017.

Such concerns lead to the development of the counter-UAV technology, which is dedicated to detect and intercept drones. It has been used for airspace protection at airports, security during large events, VIP protection, and counter smuggling at prisons [1].

The counter-UAV scenario can be modeled as a guarding territory differential game, where an intruding drone tries to enter a target area, while a group of defenders seek to intercept it. The defenders need to move in proper directions so as to get the intruder in the range of their interception devices.

The guarding territory game is a special case of pursuit-evasion games where the intruders (corresponding to the evaders in a pursuit-evasion game) also wish to enter a target area, in addition to escaping from the defenders (pursuers).

The standard way of solving a pursuit-evasion game is through the Hamilton–Jacobi–Bellman–Isaacs (HJI) equation [3]. But this equation is hard to solve due to the curse of dimensionality. Alternative efforts have been made in dimension reduction and incorporating geometric methods. For example, Chen *et al.* decomposed a 4-D problem into 2-D slices, and presented a conservative strategy for the defenders [5]. Makkapati *et al.* studied a set of sub-problems under different pursuit strategies, where the state spaces were carefully chosen such that the HJI equations were solvable [6]. Kawecki *et al.* [7] and Rzymowski [8] solved the maximal length of a line segment that one and multiple defenders can protect, by constructing a set of geometric auxiliary functions.

While the auxiliary functions were customized for the specific problems, a more general geometric concept is the dominant region (DR), which is a set of points that one player can reach before the other players. [2] The DR has been extensively used in differential game problems for strategy design [9]–[11], optimality proof [12], and player assignment in multiplayer problems [9].

Many of the works, however, assume that the capture range is zero [12], [13] or the pursuers travel faster than the evaders [15], [16] or the target area is to some extend symmetric [10], [16]. This article attempts to relax such limitations. First of all, a nonzero capture range is considered, which allows the defenders to take advantage of the large effective range of some counter-UAV techniques. Second, the speed limit on the intruder is eliminated, and both cases are covered where the intruder travels slower and faster than the defenders. Finally, the proposed strategy is applicable for any convex target area.

The essence of the proposed strategy is to find the closest point to the target area from the intruder's DR. When the defenders travel faster, the DR-based strategy is equivalent to the classic solution. When the defenders are slower, however, the classic solution is open-loop [17] and should be customized for different targets [18]. This article approximates the key property of the

Manuscript received January 7, 2020; revised March 26, 2020; accepted April 27, 2020. Date of publication May 22, 2020; date of current version August 13, 2020. This work was supported by the Natural Sciences and Engineering Research Council of Canada under its CREATE program under Grant 466088-2015. Recommended by Technical Editor Y.-J. Pan and Senior Editor X. Chen *(Corresponding author: Hugh H.-T. Liu.)*

The authors are with the Institute for Aerospace Studies, University of Toronto, Toronto, ON M3H 5T6, Canada (e-mail: flora.fu@mail.utoronto.ca; liu@utias.utoronto.ca).

Color versions of one or more of the figures in this article are available online at https://ieeexplore.ieee.org.

Digital Object Identifier 10.1109/TMECH.2020.2996901

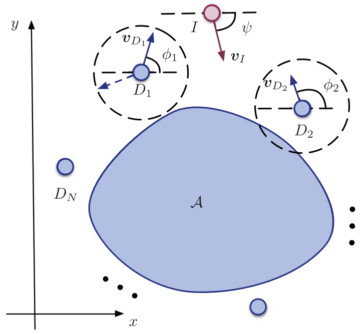

Fig. 1. Problem formulation of the guarding territory game.

classic optimal trajectory with a simple function, making the proposed strategy a closed loop and applicable in more general situations, with little loss of optimality.

The effectiveness of the proposed strategy is tested through experiment, which is rarely done in researches concerning differential games.

II. Problem Formulation

The scenario is illustrated in Fig. 1. Suppose function $g(\boldsymbol{x})$ is convex and bounded from below, and the convex target area can be described as $\mathcal{A} = \{\boldsymbol{x}|g(\boldsymbol{x}) \leq 0\}$. Because the value of $g(\boldsymbol{x})$ reflects how far point $\boldsymbol{x}$ is out from or how deep it is in the target, we will refer to it as the target level.

The group of defenders form a blockade around the target, whereas the intruder seeks to pass through the defenders and enter the target. Assume the intruder is captured once it enters any defender's interception range, i.e., $\|\mathrm{ID}_i\| < r, \exists i \in \mathbb{D}$, where $\mathbb{D}$ is the index set of the defenders.

The kinematics of the system is described by

$$\begin{aligned} \dot{x}_I &= v_I \cos\psi, \qquad \dot{y}_I = v_I \sin\psi \\ \dot{x}_{D_i} &= v_{D_i} \cos\phi_i, \quad \dot{y}_{D_i} = v_{D_i} \sin\phi_i, \ i \in \mathbb{D} \end{aligned} \tag{1}$$

where $v_k, k \in \{I\} \cup \mathbb{D}$, are velocities of the players. ψ and $\phi_i, i \in \mathbb{D}$, are heading angles and control inputs. Assume that v_I and $v_{D_i} = v_D, i \in \mathbb{D}$, are constant, and define speed ratio $a = v_D/v_I$. In the following discussion, we will use $\boldsymbol{p}_I = (x_I, y_I)$ and $\boldsymbol{p}_{D_i} = (x_{D_i}, y_{D_i})$ to represent player locations, and refer to $\boldsymbol{x} = (\boldsymbol{p}_I, \boldsymbol{p}_1, \ldots, \boldsymbol{p}_N) \in \mathbb{R}^{2(N+1)}$ as the state.

Define the regulated capture time $t_c = \min\{\bar{t}_c, t_e\}$, where $\bar{t}_c$ is the time the intruder is actually captured, and $t_e = \min\{t|\boldsymbol{p}_I(t) = \boldsymbol{p}_c = \arg\min_{\boldsymbol{p}} g(\boldsymbol{p})\}$ is the first time that the intruder reaches $\boldsymbol{p}_c$, the center of the target, where the target level is minimized. This regulation keeps t_c finite when the intruder cannot be captured.

The defenders' goal is to find strategies $\{\phi_i^*(\boldsymbol{x}), i \in \mathbb{D}\}$ that maximize the target level of $\boldsymbol{p}_I(t_c)$, whereas the intruder hopes to find strategy $\psi^*(\boldsymbol{x})$ that minimizes the same value. Assume that the $\min$ and $\max$ operations are commutable, the game can be described by the following minmax problem:

$$\min_{\psi} \max_{\phi_i, i \in \mathbb{D}} g(\boldsymbol{p}_I(t_c)). \tag{2}$$

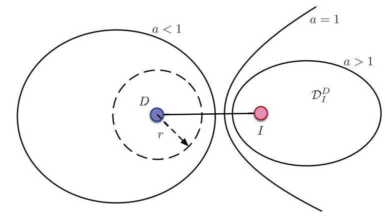

Fig. 2. DRs of one intruder against one defender.

Before presenting the solution, we state an important property of the optimal trajectories in Theorem 1, which has been proved for $r = 0$ [12], yet is generally true for kinematics that contain no state variable on the right-hand side and when $\|ID_i\| > r$ $\forall i \in \mathbb{D}$. The optimal trajectory of player $j, j \in \{I\} \cup \mathbb{D}$, refers to function $\boldsymbol{p}_j(t)$ that is solved from (1) when the optimal strategies ψ^* and ϕ_i^* $\forall i \in \mathbb{D}$ are adopted.

Theorem 1: The optimal trajectories of the guarding territory game (2) are straight lines when $\|ID_i\| > r$ $\forall i \in \mathbb{D}$.

III. Strategies for $a \geq 1$

When $a \geq 1$, a geometric solution of (2) exists based on the concept of DRs.

A. Dominant Regions (DRs)

The DR of a player is the set of points it can reach before any other players. For one intruder I and one defender D ($\|DI\| > r$), the DR of the intruder is $\mathcal{D}_I^D = \{P| \|PD\| - r \geq a\|PI\|\}$, and the DR of the defender is its complementary, i.e., $\mathcal{D}_D^I = \mathbb{R}^2 / \mathcal{D}_I^D$.

When two players are considered, the DR of the slower player is bounded. When the intruder travels no faster than the defender, its DR is convex, as shown in Fig. 2.

When there are multiple defenders, the overall DR of the intruder is the intersection of all the DRs with respect to each defender, $\mathcal{D}_I = \cap_{i \in \mathbb{D}} \mathcal{D}_I^{D_i}$, and is convex when $a \geq 1$, because each $\mathcal{D}_I^{D_i}$ is convex.

B. Optimal Strategies

With DRs, the game with $a \geq 1$ can be reformulated as an equivalent optimization problem

$$\begin{aligned} &\min_{\boldsymbol{p}} g(\boldsymbol{p}) \\ &\text{s.t.} \boldsymbol{p} \in \mathcal{D}_I, \ \ \mathcal{D}_I = \cap_{i \in \mathbb{D}} \mathcal{D}_I^{D_i}. \end{aligned} \tag{3}$$

Due to the convexity of $\mathcal{D}_I$ and g, problem (3) is convex and has a unique solution, denote by $\boldsymbol{p}^*$. It indicates the closest point to or the deepest place in the target area that the intruder can reach. Because the optimal trajectories are straight lines, the intruder's optimal strategy is to head to $\boldsymbol{p}^*$ directly.

Suppose the target is large enough such that $\boldsymbol{p}_c$ is not contained in $\mathcal{D}_I$, then $\boldsymbol{p}^*$ is at the boundary of $\mathcal{D}_I$, as shown in Fig. 3. The best that the defenders can do is to head toward $\boldsymbol{p}^*$ along straight lines, so as to capture the intruder there and ensure that it gets no closer to the target than $\boldsymbol{p}^*$.

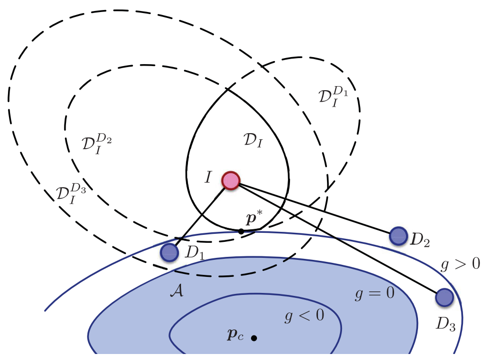

Fig. 3. Equivalent optimization problem when $a \geq 1$.

When there are multiple defenders, $\boldsymbol{p}^*$ can be out of some defenders' DRs. For example, in Fig. 3, $\boldsymbol{p}^* \notin \mathcal{D}_{D_2}^I, \mathcal{D}_{D_3}^I$. In this case, D_2 and D_3 are redundant. D_1 will capture the intruder before D_2 and D_3 arrive.

In the blockade, at least all the defenders except the two intermediate neighbors of the intruder are redundant. As a result, the multidefender game can be reduced to a two-defender problem. The intruder only needs to pass through the two closest neighbors in between.

Suppose the ith defender is not redundant, by definition of the DR, $(\|D_i\boldsymbol{p}^*\| - r)/\|I\boldsymbol{p}^*\| = v_D/v_I$. During the play, lengths $\|D_i\boldsymbol{p}^*\| - r$ and $\|I\boldsymbol{p}^*\|$ reduce at speeds of v_D and v_I, hence point $\boldsymbol{p}^*$ does not change and the trajectories are straight lines. By Theorem 1 and the property of $\boldsymbol{p}^*$, the DR-based strategies are the solution to (2).

C. Winning Conditions and the Barrier

The winner of the game is determined by the location of $\boldsymbol{p}^*$. If $\boldsymbol{p}^* \in \mathcal{A}$, the intruder wins because it can get in the target before being captured. If $\boldsymbol{p}^* \notin \mathcal{A}$, the intruder loses because it will be captured before entering the target. If $\boldsymbol{p}^* \in \partial\mathcal{A}$, the game has a neutral outcome and the intruder will be captured on the boundary of the target.

Consider the two-defender game, if locations of the two defenders are fixed, initial locations of the intruder that lead to the neutral outcome form a curve called the barrier. The intruder loses if it starts beyond, and wins if starts below. More discussions will be presented in Sections IV-E and V.

IV. Strategies for $a < 1$

When the intruder moves faster, it cannot be captured by a single defender because it has the ability to at least maintain a fixed distance from one defender. As shown in Fig. 4, the intruder can spare part of its velocity to match that of the defender, and use the rest to rotate around the defender. This strategy is referred to as the distance maintaining strategy.

Therefore, the intruder must be captured by at least two coordinated defenders simultaneously, as shown in Fig. 5. Denote by $\gamma_i = |\angle(\boldsymbol{v}_I, \boldsymbol{v}_{D_i})|, \gamma_i \in [0, \pi]$, the angle between the intruder and the ith defender's velocity vectors. When $\|ID_i\| = r, i = 1, 2$, the changing rate of the distance between each defender and the intruder is $\|\dot{ID_i}\| = v_I \cos\gamma_i - v_D$. It decreases with γ_i, and is positive when $\gamma_i < \arccos a \triangleq \gamma_0$, zero when $\gamma_i = \gamma_0$, and negative when $\gamma_i > \gamma_0$. For this reason, larger γ_i is preferable for defender i upon capture.

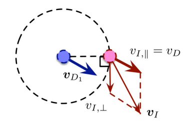

Fig. 4. Intruder's distance maintaining strategy.

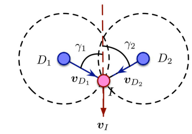

Fig. 5. Players' relative locations upon capture.

According to Theorem 1, when $a > 1$, as long as none of the capture regions is reached, the optimal trajectories are straight lines. In the event that one of the capture regions is reached, the intruder can at least maintain this distance. Although the intruder has the capability of moving away from that defender, it is not preferred. Because that way the intruder will get closer to other defenders. Having similar distances from multiple defenders is not beneficial for the intruder, because capture needs to be achieved by more than one defenders.

To prevent defenders from cooperating, and at the same time avoid capture, the intruder should conduct the distance maintaining strategy. Trajectories of the intruder and the closest defender thus start to curve. As a result, the game is divided into two stages, Phase I that all the optimal trajectories are straight lines, and Phase II that the optimal trajectories of the intruder and the closest defender are curved [17].

The standard way of solving the game is in a backward manner, i.e., Phase II is solved first, based on which the slopes of the straight line trajectories in Phase I can be obtained. But the solution of Phase II varies with the shape of the target area, and is generally hard to solve. Furthermore, such solution is a set of open-loop optimal trajectories, from which deducing a closed-loop strategy is tricky [18].

To obtain a feedback strategy, we apply the concept of DRs. For simplicity, we will be focusing on two-defender games. But the proposed strategy can be extended to multiple defenders easily, since the intruder eventually has to pass through a certain pair of defenders.

A. Target Approaching Strategy

When the intruder is faster, capture is not guaranteed. We first present a necessary condition for the intruder to win.

As shown in Fig. 6, denote by T_i the point of tangency of $\mathcal{D}_{D_i}^I$ from I. Safe directions for the intruder to go is within sector T_1IT_2. Hence, the intruder's winning condition requires $\angle T_1IT_2 > 0$.

Under this condition, a good choice for the intruder is the direction in sector T_1IT_2 with the shortest path to the target.

A simple way to compute direction $\overrightarrow{IT_i}$ can be deduced from the following theorem.

Theorem 2: Given defender D_i and intruder I ($d = \|D_iI\| > r$), $\mathcal{D}_{D_i}^I$ is the defender's DR, T_i is the point of

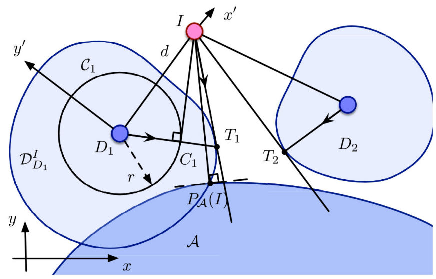

Fig. 6. Target approaching strategy of the intruder.

tangency from I to $\mathcal{D}_{D_i}^I$, and $\mathcal{C}_i$ is the boundary of the defender's capture region. Then, the following facts hold:

1) $\cos\angle T_iD_iI = r/d$;
2) connect D_iT_i, which intersects $\mathcal{C}_i$ at C_i, $IC_i \perp D_iT_i$;
3) $\angle IT_iD_i = \gamma_0 = \arccos a$.

Proof: Define reference frame $x'D_iy'$ as shown in Fig. 6. The defender D_i is at the original point, and the intruder is at $(d, 0)$. The boundary of the defender's and the intruder's DRs, $\partial\mathcal{D}_{D_i}^I$ $(= \partial\mathcal{D}_I^{D_i})$, can be described by

$$\sqrt{x'^2 + y'^2} - r = a\sqrt{(x'-d)^2 + y'^2}. \tag{4}$$

Differentiate (4) with respect to x', we have

$$\frac{x' + y'dy'/dx'}{\sqrt{x'^2+y'^2}} = a\frac{(x'-d) + y'dy'/dx'}{\sqrt{(x'-d)^2+y'^2}} \tag{5}$$

where dy'/dx' is the slope of the tangent line at point (x', y') on $\partial\mathcal{D}_{D_i}^I$, which should be equal to the slope of line IT_i. So, the function of line IT_i is

$$y' = \frac{dy'}{dx'}(x'-d). \tag{6}$$

Combining (5) and (6) and using (4), we have

$$\cos\angle T_iD_iI = \frac{x'}{\sqrt{x'^2+y'^2}} = \frac{r}{d}.$$

This proves 1) and 2) is a direct consequence of 1).

To prove 3), we first rewrite equation (4) as

$$\|D_iT_i\| - r = a\sqrt{\|D_iT_i\|^2 + d^2 - 2\|D_iT_i\|d\cos\angle T_iD_iI} \tag{7}$$

from which $\|D_iT_i\|$ can be solved as

$$\|D_iT_i\| = r + a\sqrt{\frac{d^2-r^2}{1-a^2}}. \tag{8}$$

According to the definition of the DR, we have

$$\|T_iI\| = \frac{1}{a}\left(\|D_iT_i\| - r\right) = \sqrt{\frac{d^2-r^2}{1-a^2}}. \tag{9}$$

Therefore, $\cos\angle IT_iD_i$ can be computed from the cosine law as follows:

$$\cos\angle IT_iD_i = \frac{\|D_iT_i\|^2 + \|T_iI\|^2 - \|D_iI\|^2}{2\|D_iT_i\|\|T_iI\|}. \tag{10}$$

With (8)–(9) and $\|D_iI\| = d$, one can easily check that $\cos\angle IT_iD_i = a$, which proves 3). ∎

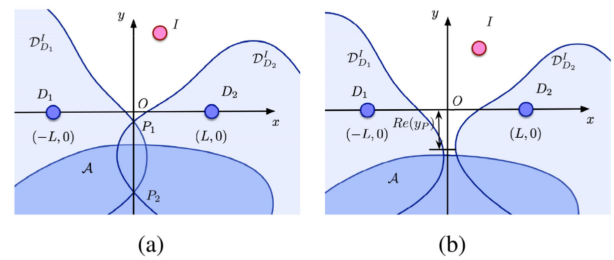

Fig. 7. DR-based strategy for $a < 1$. (a) $\mathcal{D}_{D_1}^I \cap \mathcal{D}_{D_2}^I \neq \varnothing$. (b) $\mathcal{D}_{D_1}^I \cap \mathcal{D}_{D_2}^I = \varnothing$.

With Theorem 2, T_i can be obtained by simply rotating ID_i by $\angle D_iIT_i = \arcsin r/\|D_iI\| + \pi/2 - \gamma_0$.

The target approaching strategy is only for the intruder. The defending strategy under $\angle T_1IT_2 > 0$ is the DR-based strategy described in Section IV-B.

B. DR-Based Strategies

When $\angle T_1IT_2 \le 0$, the winner of the game is uncertain. We introduce the DR-based strategy with a slight modification. First define a new reference frame as shown in Fig. 7. The original point is at the middle of segment D_1D_2, and the x-axis is along vector $\overrightarrow{D_1D_2}$. The two defenders are at $(\pm L, 0)$, whereas the intruder is at (x, y). Denote by $\mathcal{D}_{D_1}^I$ and $\mathcal{D}_{D_2}^I$ the DRs of the two defenders.

In order to reach out for the intruder simultaneously, the defenders must head to a point on the y-axis, denoted by $(0, y_P)$. Therefore

$$a\sqrt{x^2 + (y-y_P)^2} = \sqrt{L^2 + y_P^2} - r. \tag{11}$$

Equation (11) has two roots. When $\mathcal{D}_{D_1}^I \cap \mathcal{D}_{D_2}^I \neq \varnothing$, both roots are real, denoted by y_P^1 and y_P^2. Each root represents an intersection point, denoted by P_1 and P_2. Without loss of generality, assume $\|IP_1\| \le \|IP_2\|$, as shown in Fig. 7(a). Then, the defenders must head to a waypoint on segment P_1P_2. On this segment, P_1 is the best choice because it yields the largest γ_i, and has the largest target level. For the intruder, P_1 is the closest point to the target within its DR, therefore it should move to P_1 as well.

When $\mathcal{D}_{D_1}^I \cap \mathcal{D}_{D_2}^I = \varnothing$, (11) has a pair of complex roots, whose real parts indicate the location of the narrowest part of the intruder's DR, as shown in Fig. 7(b). The two defenders should head to point $(0, \mathrm{Re}(y_P))$ in hope of minimizing the distance to the intruder when it passes. The intruder should also move toward the same point in hope of breaking through safely.

C. Proximity Strategy for Defenders

When initial locations are very asymmetric, e.g., x is large, one of the capture regions will be reached first, and the game switches to Phase II. In this case, the intruder will adopt the distance maintaining strategy, and the closer defender should apply some proximity strategy accordingly. Since Phase II is hard to solve, we design a simple strategy that imitates the behavior of the optimal trajectories in [17], where two pursuers

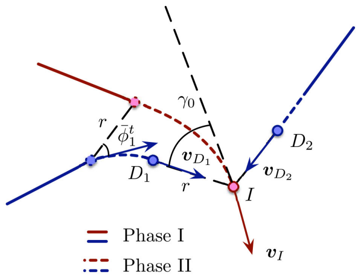

Fig. 8. Two-phase structure of the optimal trajectories [17].

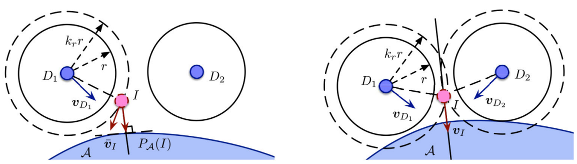

(a) (b)

Fig. 9. Intruder's proximity strategy. (a) $\| ID_1 \| \leqslant k_r r$ and $\| ID_2 \| > k_r r$. (b) $\| ID_1 \| \leqslant k_r r$ and $\| ID_2 \| \leqslant k_r r$.

seek to capture a faster evader, and the evader merely wants to escape in between, without aiming at any target area. The optimal trajectories of this game have a similar two-phase structure, as shown in Fig. 8.

At the beginning of Phase II, the closer pursuer does not head toward the evader directly, but rather gradually turns into it as the game progresses. Because the distance maintaining strategy requires the evader to spare part of its velocity to match that of the closer pursuer, this pursuer takes advantage of it and forces the intruder toward the further pursuer in the hope of cooperation.

As the game goes on, the further pursuer gets closer, capture retains higher priority, and the closer pursuer gradually allocates more speed along the line-of-sight of the evader. When capture happens, the pursuers' strategies become pure pursuit.

In the guarding territory game, the defenders play similar roles to the pursuers. Assume D_1 to be the closer defender, and $\bar{\phi}_1^t$ the angle between its moving direction and vector $\overrightarrow{D_1 I}$ at time step t, we can write $\bar{\phi}_1^{t+1} = k_\phi \bar{\phi}_1^t$, where the discount rate $k_\phi \in (0, 1)$ is a complex function of the state. We set k_ϕ to be constant as a simple approximation of the increasing emphasis on capture. Simulations suggest that $k_\phi \approx 0.98$.

D. Proximity Strategy for the Intruder

The distance maintaining strategy of the intruder is risky. If the intruder kept a precise distance of r from the closer defender, it could be captured even with minor mistakes. Hence, we allow for a buffer zone and let the intruder switch to the distance maintaining strategy when it is $k_r r$ away from the closer defender, as shown in Fig. 9(a). The closer defender adopts the proximity strategy since then accordingly.

Except avoiding capture, the intruder also endeavors to enter the target area. Without loss of generality, assume D_1 to be the closer defender, as shown in Fig. 9(a). Denote by $\bar{\boldsymbol{v}}_I$ the velocity

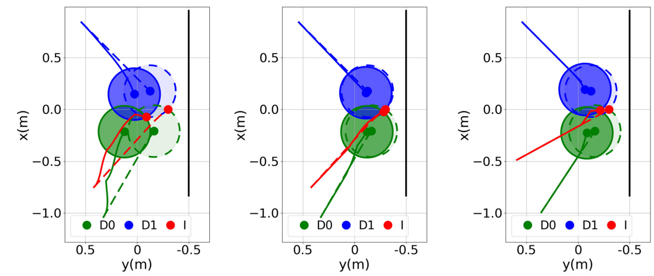

(a) (b) (c)

Fig. 10. Comparison with the classic optimal trajectories. (a) $k_r = 1.2$, with Phase II. (b) $k_r = 1.0$, with Phase II. (c) $k_r = 1.2$, without Phase II.

of the distance maintaining strategy, if it is clockwise to $\overrightarrow{IP_{\mathcal{A}}(I)}$, a better choice of the intruder is to move along the latter. Here, $P_{\mathcal{A}}(I)$ is the projection of point I on set $\mathcal{A}$.

When $k_r > 1$, the intruder can be within the buffer capture zone of both defenders, as shown in Fig. 9(b). The optimal strategy of the intruder in this case is to move along the bisector of $\angle D_1 I D_2$, whereas the defenders should apply the pure-pursuit strategy.

E. Simulations

1) Comparison With the Classic Solution: The proposed strategy is optimal when $a \geq 1$, therefore, in this section, we only verify the case where $a < 1$.

To solve the game with the classic approach, one should determine the terminal locations first, and trace backward to find the corresponding initial locations that the game starts from. What this solution presents is a set of optimal trajectories. Therefore, the classic solution is only feasible when the initial locations coincide on these optimal trajectories [18].

To verify the proposed strategy, we computed the classic optimal trajectories to find feasible initial locations, and ran the game from there using the proposed strategy. The simulation was done for two defenders with $v_D = 0.25$ m/s, $r = 0.25$ m, and $k_\phi = 0.98$. The target is a line $\mathcal{A} = \{(x, y) | y \leq -0.5\,\text{m}\}$. The results are shown in Fig. 10.

It can be seen that the trajectories of the proposed strategy (solid lines) are close to the classic solution (dashed lines), and the difference mainly comes from Phase II, because $\bar{\phi}_1^{t+1} = k_\phi \bar{\phi}_1^t$ is only a rough approximation.

To see this, the trajectories under buffer ratios $k_r = 1.2$ and $k_r = 1.0$ with the same initial locations are shown in Fig. 10(a) and (b). Because the intruder switches to the distance maintaining strategy earlier when $k_r = 1.2$, the deviation from the classic optimal trajectory is more significant.

In Fig. 10(a) and (b), the capture range of the lower defender is reached first, because the intruder's initial location is much closer to it. As a result, the distance maintaining strategy is adopted, and Phase II exits. When the initial locations are less asymmetric, e.g., in Fig. 10(c), capture ranges of the two defenders are reached simultaneously, the trajectories of the proposed strategy closely match that of the classic solution. Note that the deviation near the end of the game is due to the existence of the buffer capture zone.

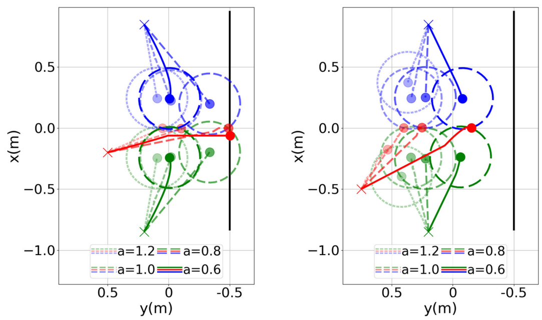

(a) (b)

Fig. 11. Trajectories under the proposed strategy for different speed ratios. (a) $\boldsymbol{p}_I = (-0.2\,\text{m}, 0.5\,\text{m})$. (b) $\boldsymbol{p}_I = (-0.5\,\text{m}, 0.75\,\text{m})$.

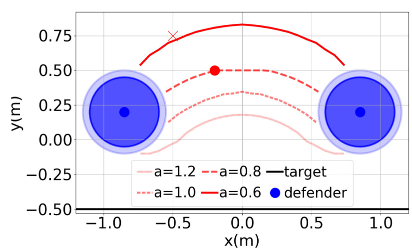

Fig. 12. Barrier under different speed ratios.

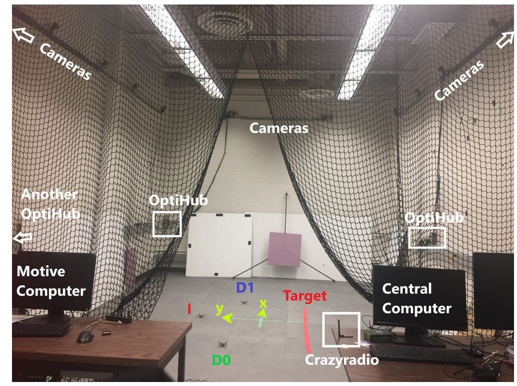

Fig. 13. Experiment setup.

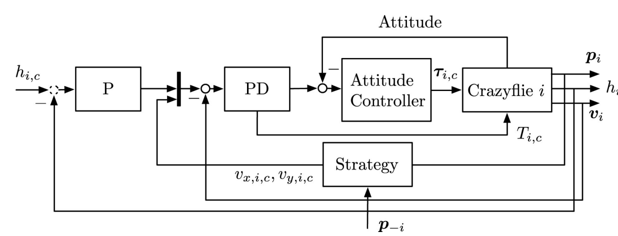

Fig. 14. Architecture of the Crazyflie 2.1 controller.

2) Impact of the Speed Ratio: By varying the intruder's speed, we further compared the performance of the proposed strategy under different speed ratios, and the results are shown in Fig. 11. As a decreases, the intruder travels faster, thus the defenders must retrograde more to block it, except the situation that the intruder is going to win, where the defenders move more actively toward the intruder, shown by the solid trajectories in Fig. 11(a).

The barrier under different speed ratios are shown in Fig. 12. The initial locations of the two defenders are at $(\pm 0.85\,\text{m}, 0.2\,\text{m})$, the same as in Fig. 11. The initial locations of the intruder in Fig. 11(a) and (b) are shown as the red dot and cross, respectively. It can be seen that the barrier of smaller speed ratios are farther from the target, therefore the intruder's winning region beneath is larger.

V. Experiments

A. Setup

The experiment was conducted on the Bitcraze Crazyflie 2.1 platform, the setup is shown in Fig. 13. Each Crazyflie had onboard sensors and a microcontroller that stabilized its attitude, and was equipped with a communication system that received thrust and attitude commands.

The location and velocity information of the Crazyflies were measured by the OptiTrack system, a high-performance optical tracking system with submillimeter accuracy.[1] In the experiment, 14 Flex 13 cameras were used and the data was processed by the Motive:Tracker software.

Data from the OptiTrack system was streamed to the central computer that ran the strategy, which took positions of all the Crazyflies and computed the heading angles. Because the magnitudes of velocities were constant, the heading angles were converted to velocity commands in x and y directions. The heights that the Crazyflies flew at were hold constant, different from each other to avoid collision. A proportional controller was used for altitude control.

The 2-D velocity from the strategy and the vertical speed from the altitude controller were fed into a velocity controller to compute the required thrust and attitude, which were sent to the Crazyflies through Crazyradios, no direct communication among the Crazyflies was implemented.

A block diagram of the architecture is shown in Fig. 14. The interface between the central computer and the Crazyflies were from the open-source code provided by Hönig and Ayanian [19].

The experiment was carried out for two defenders with initial locations $(\pm 0.85\,\text{m}, 0.2\,\text{m})$ and $k_r = 1.2$. Other parameters are the same as in the simulation.

B. Slower Intruder

We first tested the case with $v_I = 0.24$ m/s. Considering possible uncertainties of the experiment, we let both defenders play the game although one of them could be redundant.

With initial locations of the defenders fixed, we picked up a set of initial x coordinates of the intruder $\{x_I^i\}$. For each x_I^i, we ran the experiment for different initial y coordinates $\{y_I^j\}$, and observed if the intruder was captured or entered.

We initially tested each initial location twice. If the intruder was captured far from the target, and the two runs yielded same results, we labeled the corresponding initial location as 100%

[1][Online]. Available: https://v22.wiki.optitrack.com/index.php?title=Calibration#Calibration_Result_Report

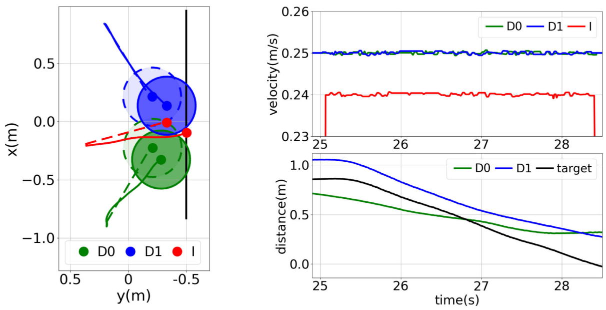

(a) (b)

Fig. 15. Experiment results for $v_D = 0.25$ m/s, $v_I = 0.24$ m/s, $x_I = -0.2$ m, and $y_I = 0.4$ m; the intruder wins. (a) Trajectories. (b) Velocities and distances.

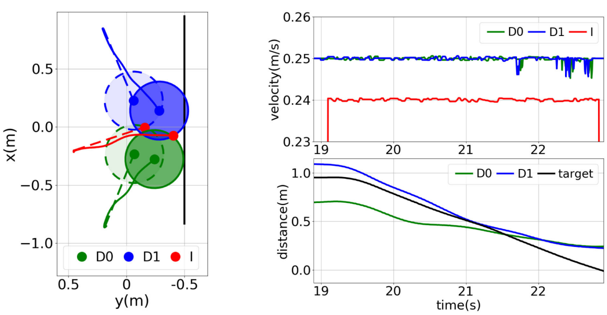

(a) (b)

Fig. 16. Experiment results for $v_D = 0.25$ m/s, $v_I = 0.24$ m/s, $x_I = -0.2$ m, and $y_I = 0.5$ m; defenders win. (a) Trajectories. (b) Velocities and distances.

capture. If the defenders were far away when the intruder reached the target, and the two runs yielded same results, we labeled the corresponding initial location as 100% entering. If neither of the conditions above were satisfied, we ran additional experiments with the identical initial locations and recorded the percentage of capture cases.

Figs. 15 and 16 show representative cases for 0% and 100% capture rates, respectively. The dashed lines are simulation results with identical initial locations for comparison. As can be seen from the figures, experimental trajectories roughly followed the simulation results, but it cost the defenders longer distances to capture the intruder. The magnitudes of the players' speeds and the distances from the intruder to the defenders and the target are shown in Figs. 15(b) and 16(b).

The experiment showed that for each x_I^i, the capture rate decreased with the y-coordinate, and both 100% and 0% capture rates were observed. If some critical y-coordinate y_I^* had 50% capture rate, the initial location (x_I^i, y_I^*) was considered to be on the barrier, i.e., if the intruder started from initial locations vertically above (x_I^i, y_I^*), it would more likely to be captured than enter the target. For each x_I^i, if the critical y-coordinate was not found from the experiment, it was estimated through linear interpolation.

Fig. 17 shows the capture rates of different initial locations tested. Each point is represented by a pie chart, where the green (red) part shows the percentage of capture (entering). The barrier solved from simulation is shown as the red dashed line for comparison. Because defenders took longer distances to capture

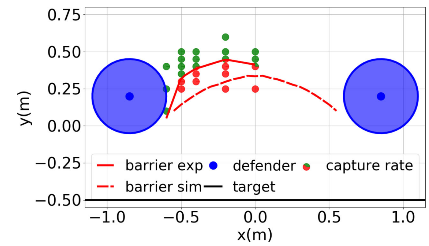

Fig. 17. Barrier for $v_D = 0.25$ m/s and $v_I = 0.24$ m/s.

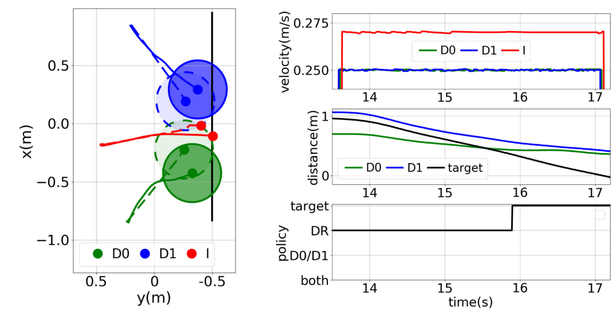

(a) (b)

Fig. 18. Experiment results for $v_D = 0.25$ m/s, $v_I = 0.27$ m/s, $x_I = -0.2$ m, and $y_I = 0.5$ m; the intruder wins. (a) Trajectories. (b) Velocities, distances, and strategies.

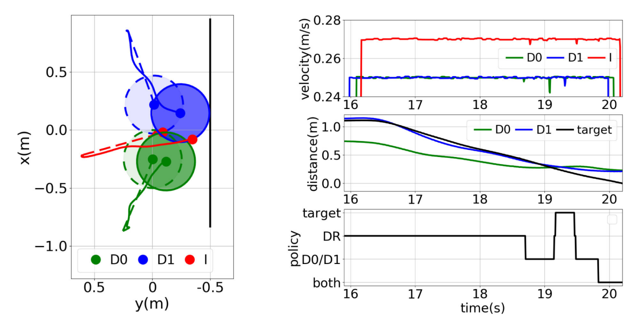

(a) (b)

Fig. 19. Experiment results for $v_D = 0.25$ m/s, $v_I = 0.27$ m/s, $x_I = -0.2$ m, and $y_I = 0.6$ m; defenders win. (a) Trajectories. (b) Velocities, distances, and strategies.

the intruder in the experiment, the barrier measured from the experiment is further away from the target area.

C. Faster Intruder

We increased the intruder's speed to $v_I = 0.27$ m/s and repeated the abovementioned procedure. Representative trajectories for entering and capture are shown in Figs. 18 and 19, respectively. Similar to the slower intruder case, capturing the intruder was more difficult in the experiment.

Since strategies for the faster intruder case are mixed, the intruder's strategies are also plotted. The four labels in the last plot of Figs. 18(b) and 19(b) represent the target approaching strategy, the DR-based strategy, and the proximity strategies with one and both defenders close.

In Fig. 18, the intruder's winning condition was met and the target approaching strategy was adopted at around 15.9 s. In Fig. 19, one of the buffer capture zones was reached around

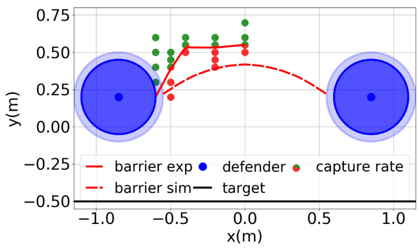

Fig. 20. Barrier for $v_D = 0.25$ m/s and $v_I = 0.27$ m/s.

18.6 s. After 0.4 s of playing the distance maintaining strategy, the intruder's winning condition was met but not kept long, after which the intruder switched back to the distance maintaining strategy. At around 19.4 s, the other defender arrives, and the intruder was captured eventually.

The barrier measured is shown in Fig. 20, which is still above that of the simulation.

VI. Conclusion

This article designs a DR-based strategy for a group of defenders to intercept a single intruder before it enters a target area. This strategy is able to handle an intruder with higher speed, allows the defenders to take advantage of their nonzero capture range, and is applicable for any convex target area. Simulation shows that the proposed strategy is close to the classic optimum, yet is more general and easier to use. The effectiveness of the proposed strategy was proved through experiment, although uncertainties and noises appeared to give advantages to the intruder.

The limitation of this article, however, is that the players are treated as massless particles during the strategy design, with the assumption that the control inputs can be followed immediately. The impact of imperfect control of actual drones can be observed in the experiment, but not further studied. We also assume a game of perfect information, where each player's location is always available to all the other players.

Although rooted in an outdoor application, this article only verified the proposed strategy through an indoor experiment. In outdoor environments, localization results and communications will be subject to much larger uncertainties, and Crazyflies are not suitable for outdoor flights. Also, the buffer ratio k_r should be more carefully tuned for different environments, and higher values are required for higher uncertainties.

Researches that address the aforementioned problems will be valuable works to improve our strategy, including incorporating quadrotor dynamics, considering imperfect information and uncertainties, verifying and improving the robustness of the proposed strategy, and conducting outdoor experiments.

References

[1] A. Holland Michel, "Counter-drone systems," Center Study Drone, Bard College, Annandale-On-Hudson, NY, USA, Feb. 20, 2018.

[2] R. Isaacs, *Differential Games: A Mathematical Theory With Application to Warfare and Pursuit Control and Optimization*. New York, NY, USA: Dover, Jan. 1999.

[3] E. Garcia, Z. E. Fuchs, D. Milutinovic, D. W. Casbeer, and M. Pachter, "A geometric approach for the cooperative two-pursuer one-evader differential game," *IFAC-PapersOnLine*, vol. 50, no. 1, pp. 15209–15214, Jul. 2017.

[4] J. F. Fisac, M. Chen, C. J. Tomlin, and S. S. Sastry, "Reach-avoid problems with time-varying dynamics, targets and constraints," in *Proc. 18th Int. Conf. Hybrid Syst., Comput. Control*, Apr. 2015, pp. 11–20.

[5] M. Chen, Z. Zhou, and C. J. Tomlin, "A path defense approach to the multiplayer reach-avoid game," in *Proc. 53rd IEEE Conf. Decis. Control*, Dec. 2014, pp. 2420–2426.

[6] V. R. Makkapati, W. Sun, and P. Tsiotras, "Optimal evading strategies for two-pursuer/one-evader problems," *J. Guid. Control Dyn.*, vol. 41, no. 4, pp. 851–862, Feb. 2018.

[7] P. Kawecki, B. Kraska, K. Majcherek, and M. Zoła, "Guarding a line segment," *Syst. Control Lett.*, vol. 58, no. 7, pp. 540–545, 2009.

[8] W. Rzymowski, "A problem of guarding line segment," *SIAM J. Control Optim.*, vol. 48, no. 2, pp. 812–838, 2009.

[9] M. Ramana and M. Kothari, "A cooperative pursuit-evasion game of a high speed evader," in *Proc. 54th IEEE Conf. Decis. Control*, Dec. 2015, pp. 2969–2974.

[10] R. Yan, Z. Shi, and Y. Zhong, "Reach-avoid games with two defenders and one attacker: An analytical approach," *IEEE Trans. Cybern.*, vol. 49, no. 3, pp. 1035–1046, Feb. 2018.

[11] L. Liang, F. Deng, Z. Peng, X. Li, and W. Zha, "A differential game for cooperative target defense," *Automatica*, vol. 102, pp. 58–71, Apr. 2019.

[12] W. Zha, J. Chen, Z. Peng, and D. Gu, "Construction of barrier in a fishing game with point capture," *IEEE Trans. Cybern.*, vol. 47, no. 6, pp. 1409–1422, Jun. 2017.

[13] D. W. Oyler, P. T. Kabamba, and A. R. Girard, "Pursuit–evasion games in the presence of obstacles," *Automatica*, vol. 65, pp. 1–11, Mar. 2016.

[14] D. W. Oyler, P. T. Kabamba, and A. R. Girard, "Dominance in pursuit-evasion games with uncertainty," in *Proc. 54th IEEE Conf. Decis. Control*, Dec. 2015, pp. 5859–5864.

[15] W. Li, "A dynamics perspective of pursuit-evasion: Capturing and escaping when the pursuer runs faster than the agile evader," *IEEE Trans. Autom. Control*, vol. 62, no. 1, pp. 451–457, Jan. 2017.

[16] S. Pan, H. Huang, J. Ding, W. Zhang, D. M. S. Vić, and C. J. Tomlin, "Pursuit, evasion and defense in the plane," in *Proc. Amer. Control Conf.*, Jun. 2012, pp. 4167–4173.

[17] P. Hagedorn and J. Breakwell, "A differential game with two pursuers and one evader," *J. Optim. Theory Appl.*, vol. 18, no. 1, pp. 15–29, 1976.

[18] H. Fu and H. Liu, "The optimal solution of a target defense game with two defenders and a faster intruder," *Unmanned Syst.*, to be published.

[19] W. Hönig and N. Ayanian, "Flying multiple UAVs using ROS," in *Robot Operating System (ROS)*. New York, NY, USA: Springer, May 2017, pp. 83–118.

Han Fu received the bachelor's degree in aerospace engineering from Shanghai Jiao Tong University, China, in 2015, the master's degree from the University of Toronto Institute for Aerospace Studies, in 2017, and transferred to Ph.D. degree, in 2018.

Her research interests include differential games, multiagent systems, and reinforcement learning.

Hugh H.-T. Liu (Member, IEEE) received the bachelor's degree in electrical engineering from Shanghai Jiao Tong University, China, in 1991, the master's degree in automation science and electrical engineering from the Beijing University of Aeronautics and Astronautics, China, in 1994, and the Ph.D. degree in mechanical engineering from the University of Toronto, Canada, in 1998.

He is currently a Professor with the Institute for Aerospace Studies, University of Toronto. His research interests include autonomous unmanned systems, cooperative and formation control, fault-tolerant control, active control on advanced aircraft systems, and integrated modeling and simulations.